A Discontinuous Galerkin Method To Solve Maxwell Equations In Time Domain

E. Montseny[1], S. Pernet[2], X. Ferrieres[3], M. Zweers[3], G. Cohen[4] and B. Pecqueux[5]

[1] LAAS-CNRS, 7 avenue du colonel Roche, 31055 Toulouse
[2] CERFACS, 42 avenue Gaspard Coriolis, 31057 Toulouse, France
[3] ONERA DEMR, unité CDE, 2 Avenue Edouard Belin, 31055 Toulouse, France
[4] INRIA, Domaine de Voluceau, BP 105, Rocquecourt, 78153 Le Chesnay cedex, France
[5] DGA, Centre d'Etudes de Gramat, France

Abstract: In this paper, we describe a high-order spatial Discontinuous Galerkin approach to solve Maxwell's equations in the time domain. This approach is based on the use of hexahedral meshes and on a judicious choice for the approximations spaces. This results in an efficient solver in terms of storage and CPU time, for any order of approximation.

1. Introduction

Many EMC require the knowledge of the electromagnetic fields near the structure or inside cavities where the cables are routed. To satisfy these constraints in the simulations, the proposed numerical schemes have to demonstrate low numerical dissipation and dispersion, and have to take into account curved geometries. In all the schemes used to solve the Maxwell-problem [1][2], we recently find a class of numerical schemes, the so-called Discontinuous Galerkin (DG) methods, [3][5][4] which permit us to use a large family of elements and which have a very accurate approximate solution. This kind of methods also offers a lot of possibilities in terms of numerical scheme which in the future will make easier to process the local refinements, the boundary conditions, the non linear aspects, ... In this paper, we describe a particular high-order spatial DG method, with the main advantages of low storage for Mass and Stiffness matrices and a fast resolution in terms of CPU time, for all orders of approximation.

2. The mathematic formulation

To introduce our DG method, we consider the electromagnetic problem, described in a domain Ω by the Maxwell equations :

$$\varepsilon \frac{\partial E}{\partial t} + \sigma E = \nabla \times H, \tag{1}$$

$$\mu \frac{\partial H}{\partial t} = -\nabla \times E, \tag{2}$$

$$E(x,0) = E_0(x), \quad H(x,0) = H_0(x) \text{ on } \Omega, \tag{3}$$

where (E, H) are the electric and magnetic fields and $\mathbf{n}$ the outward normal to the boundary of Ω. ε, σ and μ are the permittivity, conductivity and permeability matrices. In this model, on the boundary $\partial\Omega$ of the domain, to simulate unbounded space we use a PML formalism where a condition $n \times E = 0$ ends the layers.

Let $\mathscr{T}_h$ be a hexahedral mesh of Ω such that $\Omega = \bigcup_{i=1}^{N_e} K_i$. In our approach, for each $K_i \in \mathscr{T}_h$, we rewrite (1), (2) and (3) by adding terms which define the jumps of the tangential electric and magnetic components accross the boundary of K_i. We obtain on K_i :

$$\begin{aligned}\int_{K_i} \varepsilon \frac{\partial E}{\partial t} \cdot \boldsymbol{\psi}\, dx + \int_{K_i} \sigma E \cdot \boldsymbol{\psi}\, dx = \int_{K_i} \nabla \times H \cdot \boldsymbol{\psi}\, dx + \alpha \int_{\partial K_i} [\![H \times \mathbf{n}]\!]_{\partial K_i}^{K_i} \cdot \boldsymbol{\psi}\, ds \\ +\beta \int_{\partial K_i} [\![\mathbf{n} \times (E \times \mathbf{n})]\!]_{\partial K_i}^{K_i} \cdot \boldsymbol{\psi}\, ds,\end{aligned} \tag{4}$$

$$\begin{aligned}\int_{K_i} \mu \frac{\partial H}{\partial t} \cdot \boldsymbol{\phi}\, dx = -\int_{K_i} \nabla \times E \cdot \boldsymbol{\phi}\, dx + \gamma \int_{\partial K_i} [\![E \times \mathbf{n}]\!]_{\partial K_i}^{K_i} \cdot \boldsymbol{\phi}\, ds \\ +\delta \int_{\partial K_i} [\![\mathbf{n} \times (H \times \mathbf{n})]\!]_{\partial K_i}^{K_i} \cdot \boldsymbol{\phi}\, ds,\end{aligned} \tag{5}$$

where α, β, γ, δ are positive constants, $\boldsymbol{\phi} \in [H(\mathscr{T}_h)]^3$, $\boldsymbol{\psi} \in [H(\mathscr{T}_h)]^3$ and $[\![\mathbf{v}]\!]_{\partial K_i}^{K_i}$ is the jump of a vector-valued function $\mathbf{v}$ across the boundary of K_i. $H(\mathscr{T}_h)$ defines the functional space given by $\{v \in L^2(\Omega); \forall K \in \mathscr{T}_h, v_{|K} \in H^1(K)\}$.
Now we choose α, β, γ and δ so that the last formulation (4)-(5) is equivalent to the Maxwell's equations (1)-(3) and to ensure a well posed problem, the energy $\varepsilon \int_\Omega E \cdot E\, dx + \mu \int_\Omega H \cdot H\, dx$ of this new formulation must be bounded in time.

A study of the energy of (4)-(5) for $\sigma = 0$ shows that this system is dissipative for $\beta \geq 0$, $\delta \geq 0$ and $1 + \alpha - \gamma = 0$. Moreover, if $\beta = \delta = 0$, we get an energy conservation. So, in order to obtain a non-dissipative formulation and two equivalent problems, we set $\beta = \delta = 0$ and $-\alpha = \gamma = \frac{1}{2}$ for any interior face and $\gamma = 1$ and $\beta = \delta = \alpha = 0$ on a metallic face.

Now, let $\hat{K} = [0, 1]^3$ be the unit cube and a hexaedric cell $K_i \in \mathscr{T}_h$, $\mathbf{F}_i$ is a trilinear conform mapping such that $\mathbf{F}_i(\hat{K}) = K_i$. DF_i defines its Jacobian matrix and $J_i = \det(DF_i)$. The approximate problem is then defined in the following approximation of $[H(\mathscr{T}_h)]^3$:

$$\mathbf{V}_h^r = \{\mathbf{v} \in [L^2(\Omega)]^3 \text{ such that } |Ji| DF_i^{-1} \mathbf{v}|_{K_i} \circ F_i \in [Q_r(\hat{K})]^3\}, \tag{6}$$

where $Q_r(\hat{K})$ is the set of polynomials of order less or equal to r in each variable. In the following, we shall call a Q_r approximation for the Discontinuous Galerkin method, an approximation based on $\mathbf{V}_h^r$.

1.1. Basis Functions

To define the basis functions of $\mathbf{V}_h^r$, first, we define local basis functions on $\hat{K}$. Let $\hat{\vec{\xi}}_{i,j,k} = \left(\hat{\xi}_i, \hat{\xi}_j, \hat{\xi}_k\right)$, $0 \leq i \leq r$, $0 \leq j \leq r$, $0 \leq k \leq r$, be a set of points of $\hat{K}$, where $\hat{\xi}_\ell$ represents a Gauss quadrature point on the interval $[0, 1]$. We define the set of the $(r+1)^3$ Lagrange interpolation polynomials $\theta_{i,j,k} \in Q_r$ such

that $\theta_{i,j,k}(\hat{\vec{\xi}}_{\ell,m,n}) = \delta_{i\ell}\delta_{jm}\delta_{kn}$, where δ_{ij} is the Kronecker symbol. Then, we define the following set $\widehat{\mathscr{B}}$ of vector-valued basis functions on $\hat{K}$: $\boldsymbol{\theta}^{(1)}_{i,j,k} = (\theta_{i,j,k}, 0, 0)^T$, $\boldsymbol{\theta}^{(2)}_{i,j,k} = (0, \theta_{i,j,k}, 0)^T$, $\boldsymbol{\theta}^{(3)}_{i,j,k} = (0, 0, \theta_{i,j,k})^T$. Fig.1 shows the location of the degrees of freedom in $\hat{K}$ for a Q_3 approximation.

Finally, for each hexahedron K_ℓ we define $3(r+1)^3$ functions $\boldsymbol{\phi}^{(n)}_{\ell,i,j,k}$ of the basis $\mathscr{B}_v$

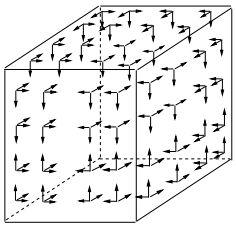

Figure 1. Degrees of freedom for Q_3 approximation on the unit cube.

of $\mathbf{V}^r_h$ such that $\boldsymbol{\phi}^{(n)}_{\ell,i,j,k} \circ \mathbf{F}_\ell = DF_\ell^{*-1}\boldsymbol{\theta}^{(n)}_{i,j,k}$.

1.2. Discrete Formulation

In problem (4)-(5), by using the above definitions of basis functions to approach the fields and by computing all the integral by the Gauss rule, we get the following discrete formulation of the problem, whith a leapfrog scheme in time :

$$B_\varepsilon \frac{\mathbf{E^{n+1}} - \mathbf{E^n}}{\Delta t} + B_\sigma \frac{\mathbf{E^{n+1}} + \mathbf{E^n}}{2} + R_h \mathbf{H^{n+1/2}} + \alpha\, S_h \mathbf{H^{n+1/2}} + \mathbf{J^{n+1/2}} = 0, \tag{7}$$

$$B_\mu \frac{\mathbf{H^{n+1/2}} - \mathbf{H^{n-1/2}}}{\Delta t} + R_h \mathbf{E^n} + \gamma\, S_h^* \mathbf{E^n} = 0, \tag{8}$$

In this system

- B_ε, B_σ, B_μ are 3×3 block-diagonal symmetric mass matrices. This property comes from the orthogonality of the basis functions and a adequate numbering of the degrees of freedom ;
- the stiffness matrix R_h and the jump matrices S_h, S_h^* are very sparse and require almost no storage. Only the storage of the integral terms computed on the reference element $\hat{K}$ and the value of the sign of J_i on each element K_i are necessary. This is due to the somehow strange definition of $\mathbf{V}^r_h$ which induces the following properties :
  For any $\boldsymbol{\phi} \in \mathbf{V}^r_h$, $\boldsymbol{\psi} \in \mathbf{V}^r_h$ such that $\boldsymbol{\phi} \circ \mathbf{F}_\ell = DF_\ell^{*-1}\hat{\boldsymbol{\phi}}$ and $\boldsymbol{\psi} \circ \mathbf{F}_\ell = DF_\ell^{*-1}\hat{\boldsymbol{\psi}}$, we have
  $$\int_{K_i} \nabla \times \boldsymbol{\phi} \cdot \boldsymbol{\psi}\, dx = signJ_i \int_{\hat{K}} \hat{\nabla} \times \hat{\boldsymbol{\phi}} \cdot \hat{\boldsymbol{\psi}}\, dx$$
  and
  $$\int_{\partial K_i} (\boldsymbol{\phi} \times n_i) \cdot \boldsymbol{\psi}\, d\sigma = signJ_i \int_{\partial \hat{K}} (\hat{\boldsymbol{\phi}} \times \hat{n}) \times \hat{\boldsymbol{\psi}}\, d\hat{\sigma}$$

where $\hat{\nabla}$ is the the gradient operator on $\hat{K}$. In the numerical scheme, the block-diagonal structure of B_ε, B_σ and B_μ leads to a quasi explicit scheme of resolution in time without the need to store big inverse mass matrices. In particular, this induces a fast method ($O(r^4)$ number of operations per iteration). So, this approach allows us to have a high order spatial approximation with a low memory storage $(24(r+1)^3+1$ value to store by cell for a Q_r approximation).

3. Numerical Results

To illustrate the advantages of this method versus classical electromagnetic methods like the yee's scheme [1], we present in this section some comparisons to :

- the propagation of a mode inside a cavity for important number of wavelenghts
- the evaluation of a scattered field near an objects with an important curved geometry.

2.1. Propagative problem inside a cavity

Let a cubic cavity with a $1m$ lenght, be perfectly metallic. We wish study the propagative mode (3,0,0) whose the analytical solution is given by :

$$\begin{cases} E_x = E_y = H_z = 0 \\ E_z = sin(3\pi(x-x_0))sin(3\pi(y-y_0))cos(\omega t) \\ H_x = \frac{3\pi}{\omega\mu_0} sin(3\pi(x-x_0))cos(3\pi(y-y_0))sin(\omega t) \\ H_y = \frac{3\pi}{\omega\mu_0} cos(3\pi(x-x_0))sin(3\pi(y-y_0))sin(\omega t) \end{cases} \tag{9}$$

With $\omega = c_0\, 3\,\pi\,\sqrt{(2)}$ and (x_0, y_0, z_0) the center of the cavity. Figure 2 and Table 1 show comparison results between FDTD and DG methods. On these results, we notice the gain in terms of storage and CPU time of the DG method. In this example by using a high spatial approximation with the DG method, we need, only, to mesh the cavity by using $3 \times 3 \times 3$ cells.

Table 1. Costs in terms of memory and CPU time.

Method	*CPU time*	*Memory*
FDTD $\lambda/10$	40s	1.5Mo
FDTD $\lambda/20$	2mn	5Mo
FDTD $\lambda/30$	5mn	12Mo
FDTD $\lambda/40$	14mn	27Mo
GD Q5	4mn17s	2Mo
GD Q6	7mn10s	2.7Mo

2.2. scattered problem

In scattering problem, the use of high order DG method can be interesting for size

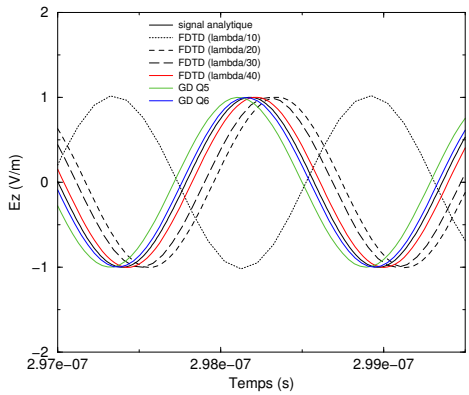

Figure 2. Comparison FDTD/DG at the center of the cavity.

of the mesh and accuracy on the solution. For example, let a flat cone be perfectly metallic and illuminated by a plane wave. We want to evaluate the field near the cone located at the point A of the figure 3.

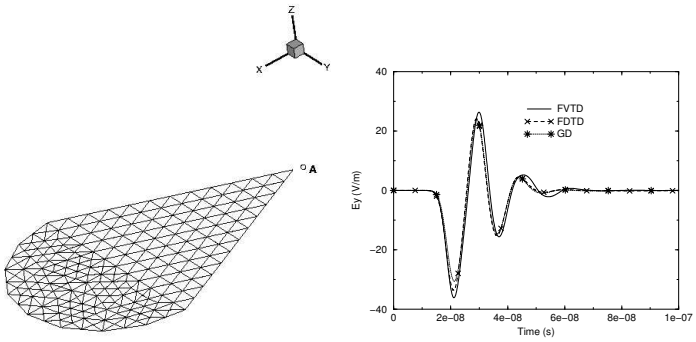

Figure 3. Comparison between FDTD and DG methods.

Figure 3 shows also some comparisons between differents methods. To obtain a similar result in terms of accuracy, we need to use for the FDTD method a mesh where the size of the cell is of order $\lambda/40$ and a time step $dt = 4.e-11s$. In these conditions, w obtain a CPU time equal to $99mn$ with a memory storage given by $27Mo$. For the DG method, by using a Q_3 approximation, with a time step equivalent to the FDTD, we obtain a CPU time equal to $25mn$ with a memory storage of $15Mo$. We note also on this simple example the possible interest to use a high order DG method to solve the problem, even if other second order schemes like FDTD or also FVTD could be more attractive in scattered problems.

The advantage of this method is strongly related to the use of an hexahedral mesh. Unfortunately, such meshes introduce a practical difficulty. In fact, hexahedral meshes are not easy to generate, contrary to tetrahedral meshes. A solution to this problem consists to construct an hexahedral mesh by using a tetrahedral one in which

each tetrahedron is split into four hexahedra. This method, enables us to apply our DGM approach for very complex structures, but the meshes obtained have very irregular elements which imply a small step time to ensure stability of the scheme. In addition to this constraint, the use of a conservative scheme for our Discontinuous Galerkin approach induces a lot of parasitic waves which are more important in this kind of mesh than for regular meshes and the solution can be very distorted. To improve these points, we introduce in our scheme the damped terms of the fluxes $(n \times (E \times n), n \times (H \times n))$ with a small factor (0.01) and we take into our scheme a local time-stepping method.

3. Local time-stepping

Generally, the unstructured meshes of the objects obtained in our simulation models have a large variety of cell size. In these conditions, using the time step which ensure the stability of the numerical scheme on the whole computational domain, is too stringent. Different research works have been done in order to obtain a local time-stepping stable method. In particular, a symplectic scheme seems to present advantage to ensure stability [6]. In addition, this scheme permits to treat the entire problem as a set of cell area classes for which a local time step is given. Then, the evolution of the fields in time can be easily done by a recursive process. The symplectic scheme proposed for Maxwell's equations is based on the Verlet scheme [7]. However, the requirement field values at times which are not computed implies the lost of the symplectic property of the scheme proposed. For this reason and because the Yee scheme is less CPU time consuming than the Verlet scheme, we have developped a local time-stepping approach based on the Yee scheme. So far, we don't ensure the stability of this approach by a condition on the time step, but the behaviour of our approach on long time is similar to the approach based on the Verlet's scheme. The recursive scheme developped can be explained as :

- take n as the number of classes found for our mesh
- **avanceH**(n); **avanceH**(n)

The subroutine **avanceH** can be written :

- if (n=1) then **EvalH**
- else
  - $dt = 3^{n-1} dt_{min}$
  - **EvalH**
  - **avanceH**($n-1$); **avanceE**($n-1$); **avanceH**($n-1$)

For the subroutine **avanceE** we have :

- if (n=1) then **EvalE**

- else
  - $dt = 3^{n-1}dt_{min}$
  - **EvalH**
  - **avanceE**$(n-1)$; **avanceH**$(n-1)$; **avanceE**$(n-1)$

In these subroutines, **EvalH** and **EvalE** define respectively, the evaluation of the magnetic and electric fields by using Yee's method.

In this local time-stepping method, we define the smallest time step dt_{min} which ensures stability for all the cells and, for each cell, we define the local time step which verifies the stability condition. Then, we define n different classes with local time step equal to $3^{n-1}dt_{min}$ in ranging from the smallest to the largest time step.

To evaluate this local time-stepping method, we present a comparison in terms of CPU time between four approaches. The first approach noted *scheme0* is the DG method without local time-stepping method. The second approach noted *scheme1* is a local time-stepping method using two local time steps and two classes of elements. The third approach noted *scheme2* is the local time-stepping approach based upon the Verlet scheme. Finally, the fourth approach noted *scheme3* is the method proposed with the Yee scheme. The examples taken into account for the comparisons are an airplane and the GENEC cavity whose meshes are given in Figure 4. The tables 2

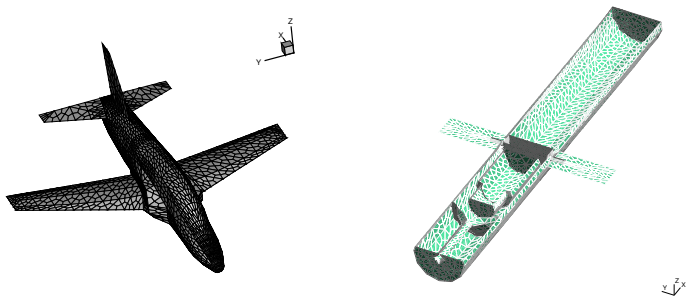

Figure 4. Meshes of the objects studied.

and 3 give the results obtained respectively for the airplane and the GENEC example. The number of classes found for the airplane is $N = 7$ with *scheme2* and $N = 5$ with *scheme3*. For the GENEC we find respectively $N = 10$ with *scheme2* and $N = 6$ with *scheme3*. We can see the advantage of the method proposed.

Table 2. Gain in time for the airplane example.

scheme0	*scheme1*	*scheme2*	*scheme3*
1	2.5	4.5	5.5

Table 3. Gain in time for the GENEC example.

scheme0	*scheme1*	*scheme2*	*scheme3*
1	2.7	11	15

4. Conclusion

In this paper, we presented a high spatial order Discontinuous Galerkin method which ensures a very accurate solution with a low memory storage and a low CPU time. This method is based on a spatial non dissipative scheme and on an approximation upon mesh constituted of hexahedra. This particularity permits to obtain easily high degree of spatial approximation by cartesian products. The obtention of such meshes can be done by splitting tetraedric cells of a non-structured classical mesh into 4 hexaedric cells. This possibility makes the method very attractive even for complex geometries and in particular for cavity problems and for problems where the signals are unsteady during a long time. However, the size of some local cells into the splitted mesh imposes a very small time step for the method in order to ensure its stability. Actually, to correct this lack of performance, a local time step method has been studied and introduced in the method. The gains obtained are very promising.

References

[1] K.S. Yee, "Numerical solution of initial boundary value problems involving Maxwell's equations in isotropic medium",IEEE Trans. Antennas Propag., Vol. 14, No .3, pp. 302-307,May,1966.

[2] P. Bonnet & al, "Numerical modeling of scattering problem using a time finite volume method", JEMWA, Vol. 11, pp. 1165-1184, 1997.

[3] J.S. Hesthaven, T.C. Warburton, "Nodal high-order methods on unstructured grids. I. Time-domain solution of Maxwell's equations", Journal of Computational Physics, **181**, No. 1, pp. 186-221, 2002.

[4] S. Piperno and L. Fezoui, "A centered Discontinuous Galerkin finite volume scheme for the 3D heterogeneous Maxwell equations on unstructured meshes", INRIA Research Report No. 4733, Feb. 2003.

[5] G.Cohen, X.Ferrieres, S.Pernet, "A spatial high-orderhexahedral discontinuous Galerkin method to solve Maxwell's equations in time domain", Journal of Computational Physics 217 (2006) pp. 340-363.

[6] S. Piperno, "Symplectic local time-stepping in non dissipative DGTD methods applied to wave propagation problem", rapport INRIA,No. 5643, july 2005.

[7] D.J.Hardy, "Symplectic variable step-size integration for N-body problems", Proceeding of the NSF/CBMS, regional Conference on Numerical Analysis of Hamiltonian Differentiel Equations, Vol. 29, pp. 19-30, 1999.